# Numerical Investigation of Micro Hole Film Cooling Performance

Sana Abd Alsalam[*] and Bassam Jubran

*Aero-Thermal Management Laboratory, Department of Aerospace Engineering,*
*Ryerson University, 350 Victoria St., Toronto, Ontario, Canada, M5B2K3*

## Abstract

Micro hole film cooling is an air-cooling technology and a new approach to improve the cooling performance and the thermal protection of turbine blades. This paper is a numerical study focuses on the effect of the blowing ratio and the freestream turbulence intensity on film cooling performance of a single round micro cooling hole with a 200 µm diameter on a flat plate model. The computation is performed on FLUENT-ANSYS to predict the film cooling effectiveness performance as well as the thermal and flow fields at various blowing ratios. The main findings of the analysis are that (1) the optimal cooling performance is attained at low blowing ratios, (2) in contrast to the cylindrical macro hole, the circular micro hole showed about 30 % increase in the averaged overall film cooling performance with approximately a 12 % reduction in the coolant blowing ratio at the highest averaged lateral film cooling effectiveness, (3) high freestream turbulence intensity causes an increase in the lateral average film cooling effectiveness while it has a minor effect on minimizing the centerline effectiveness.

**Keywords:** *Film cooling; Micro hole film cooling; Film cooling effectiveness; Numerical simulation.*

## Nomenclature

| | |
|---|---|
| CFD | Computational Fluid Dynamics |
| D.R | Density ratio |
| $D_M$ | Macro hole diameter |
| $D_m$ | Micro hole diameter |
| L | Lateral distance in the spanwise direction |
| L/D | Length to diameter ratio of the cooling hole |
| M | Blowing ratio or mass flux ratio |
| P/D | Pitch to diameter ratio of the cooling hole |
| T | Temperature |
| V | Velocity |
| X/D | Downstream distance of the cooling hole |
| Y+ | Normalized distance from the wall |

### Greek symbols

| | |
|---|---|
| η | Centerline adiabatic effectiveness |
| $\bar{\eta}$ | Laterally averaged effectiveness |

### Subscripts

| | |
|---|---|
| c | Coolant |
| ∞ | Freestream |
| aw | Adiabatic wall |

### Acronyms

| | |
|---|---|
| AITEB II | Aerothermal Investigations on Turbine End-Walls and Blades II |
| CRVP | Counter-Rotating Vortex Pairs |
| EDM | Electrical discharge mechanism |
| EWT | Enhanced wall treatment |
| FSTI | Freestream turbulence intensity |
| MTJ | Micro-Tangential Jet |
| RANS | Reynolds-Averaged Navier-Stokes |
| RKE | Realizable k-ε turbulence |
| SIMPLEC | Semi-Implicit Method for Pressure-Linked Equations-Consistent |

## 1. Introduction

Gas turbine engines continue to strive towards a better performance, whereby the highest engine thermal efficiency and power output can be obtained by operating the engine at a higher turbine inlet temperature [1]. This temperature in today's engine reached about 2000 K [2], which exceeds the metallurgical limit of the turbine blades. Thus, it is importance to protect the turbine blade

working in such a harsh environment to avoid thermal and structure failure. Despite the improvement in materials technology and the use of the thermal barrier coating to enhance the thermal protection of the turbine blades, the best thermal performance can be achieved by utilizing different cooling techniques. Film cooling is one of the most common and efficient cooling methods have been applied to real turbine blades. Whereas a relatively cool air that retrieved from the compressor; relative to the mainstream, is injected from single/multiple holes on the blade surface to produce a thin layer of a coolant jet that prevent the direct contact of the surface with the mainstream and reduce the heat transfer to it [3, 4]. A typical amount of compressed air used as a coolant for the turbine alone is nearly 20-30%, which is considered a loss and penalty to the thermodynamic cycle [5]. Thus, controlling and limiting the amount of cooling air is necessary while maintaining the temperature of the blade surface within the limit of maximum blade temperature [6]. Therefore, the film cooling research that focuses on lowering the amount of coolant while using it effectively will have great potential for improving the air-cooling technology.

Film cooling performance is strongly dependent on coolant to mainstream flow condition such as the mass flux ratio (blowing ratio), and mainstream turbulence intensity. Whereby in the actual engine operating conditions, the flow upstream the turbine is mostly featured by a high level of freestream turbulence intensity (FSTI) that exceeds a 20 %, and a large-scale of turbulent structure which changes the mixing and penetration of the freestream with the coolant jet specifically near the injection location [7]. For more than half a century now, most of the research efforts conducted, both experimentally and numerically, are related to the film cooling performance from a discrete/row of a cooling hole(s) at a macro size, and more research is still underway. Bogard and Thole performed an extensive review of the available film cooling literature on macro-scale film cooling with the influence of many key parameters on the cooling performance [8]. They pointed out that the classical film cooling problem of the cylindrical hole under relatively simple flow conditions can be reasonably predicted with a CFD, and its cooling performance is dependent on the blowing ratios [8]. Recently, Acharya and Kanani reported in details the state of art of the film cooling for both a flat plate and curved turbine blade that summarized more than a hundred sixty research papers [9]. They stated that the blowing ratio and freestream turbulence intensity have a high impact not only on the film cooling effectiveness but also the thermal and flow field [9]. The turbulence intensity effect on film cooling effectiveness for a simple macro round hole is very well known [10 – 16], whereas at low to moderate blowing ratios, the centerline effectiveness decreased by increasing the freestream turbulence intensity while at high blowing ratio the lateral effectiveness is increased [10-16].

There is a growing interest recently in evaluating the micro scale film cooling performance as an effective technique to cool the next generation of a high-performance turbine engine. It was found that micro holes offer a promising cooling performance with less coolant consumption, which is the key factor in improving engine performance. This is also very much motivated by the fast-paced advancements in today's manufacturing and material technology. It has been reported that micro cooling hole could be produced with high accuracy at a reasonable cost using a laser drilling or electrical discharge mechanism (EDM) on a single crystal superalloy whereby the hole diameter can be less than a hundred micrometre [17, 18]. Besides using the additive manufacturing technique that considered to be the new revolution in gas turbine industry that could fabricate not only a small hole in the micro size but also a very complicated hole geometry [9, 19].

Early studies on micro/effusion hole cooling were first proposed to overcome the structure and mechanical strength limitations of the transpiration cooling [20]. In which the coolant jet in transpiration cooling is normally injected to the blade surface through a porous wall with an average of a pore diameter 10-50 µm and wall thickness 1 mm, that would achieve a full uniform continues coolant coverage and high cooling effectiveness. Those benefits of the transpiration cooling come at the cost of making the structure of turbine blades not sufficient enough to maintain the engine durability goals, and this is the main reason of why the transpiration cooling was not matured [20].  Accordingly, with the micro hole cooling, it is expected to achieve the great benefit of film cooling whereas the coolant remains very close to the blade surface with less mixing with the freestream while maintaining the structure and mechanical strength of the turbine blade. Banker [21] argued that all of the gas turbine blades in today's commercial operation still use the conventional macro hole film cooling, but they have many weaknesses and limitations and tend to be more complex to achieve high performance. Therefore, he suggested that moving towards the micro hole cooling concept would be a simple solution for reducing the amount of coolant while producing a better uniform distribution and maintaining it close to the surface. He also pointed out that the micro hole currently could face some challenges to be implemented in a real turbine engine blades because of the possible risk of the hole blocking and the manufacturing constraints. Moreover, the outcomes of AITEB II research project has revealed that there could be about 10% saving of coolant flow, 1.5 increasing engine efficiency, and 1%  reduction in $CO_2$ emissions by applying highly efficient cooling technologies such as advanced micro-hole cooling [22].

Table 1 shown below, presents the research efforts that have been made up to date both numerically and experimentally on the micro hole(s)/slot(s) film cooling in comparison to the current study. It is clear from this table that there is a lack of a detailed analysis of the film cooling performance and its thermal and flow fields from a single micro cylindrical hole; which is the most convenient shape of cooling holes, under engine like operating conditions. Green study was focused on the possibility of the hole blocking at a range of blowing ratios (0.25 - 1.0), and it was reported that increasing the turbulence intensity of the mainstream caused an increase in particle deposition on the plate surface [23]. Also, It was reported the non-existence of the counter-rotating vortices structure in the micro hole flow field [23]. Sriram and Jagadeesh [24] and Gerdroodbary et al.[25] concluded that film cooling effectiveness for an array of micro-cooling jets was much better than that of a single macro jet, and the array of microjets has about 50 % reduction of the surface heat transfer as well as a 37% reduction of the coolant jet consumption [24]. Li et al.  [26] found a good film cooling effectiveness from the micro slot, especially with proper control of the slot height, as well as a decrease of the coolant air consumption at least twofold than that for the macro slot. Hassan and Hassan revealed that the micro tangential slot exhibited excellent cooling effectiveness on both the pressure and suction side of the turbine van and the effectiveness increases by increasing the blowing ratio [27]. Balasubramaniyan and Jubran initiated a CFD analysis of film cooling effectiveness for a single round micro hole, and they found that micro hole has high centerline effectiveness in the hole vicinity region and a wider coolant spreading in the spanwise direction [28]. However, the study was limited to two blowing ratios (M=0.5 and 1.0) at FSTI= 1% [28]. More recently, Ochrymiuk [29] reported a significant decrease in the coolant usage which was about 72.8 % for a micro-holes with a 100 µm diameter at M=1.0 in contracts to that of the macro cooling holes while keeping the same level of the average value of cooling efficiency.

Table 1. The Summary of micro hole film cooling conducted research.

| Authors | type of study | Hole Shape | Hole diameter | L/D | M | α | FSTI | Data obtained |
|---|---|---|---|---|---|---|---|---|
| Green [23] | Numerical/flat plate model. | Single round hole / multiple holes (row of five holes) | 70 µm | 17.14 | 0.25-1.0 | 90° | 5% & 20% | Single hole: Particle trajectories for the possibility of the hole blocking. Multiple holes: velocity profile, temperature distribution, and Particle trajectories |
| Sriram and. Jagadeesh [24] | Experimental/ blunt cone model at hypersonic Mach numbers | Slot single jet/ an array forward-facing of micro-jets | 2 mm & 0.9 mm)/ 300 µm | - | - | - | - | For same effective area: heat transfer rate, Stanton number, and the images of the flow field |
| Gerdroodba ryet al. [25] | Numerical/ blunt cone model at hypersonic Mach numbers | Slot single jet/ an array of forward-facing of micro-jets | 2 mm & 0.9 mm)/ 300 µm | - | - | - | - | For same effective area: flow structure, mass fraction and temperature distribution, and heat load reduction. |
| Li et al. [26] | Experimental/ flat plate model. | Slot | (slot heights of 25 µm, 45 µm and 50 µm | - | 1-12.5 | 90° | 1.0 % | Film effectiveness |
| Hassan and Hassan [27] | Experimental/ micro tangential Jet on a gas turbine vane | Circular supply micro tube and a shaped exit parallel to the vane surface. 13 holes on the pressure side and 11 on the suction | 600 µm | 2.5 | 0.5 -1.5 (pressure side) 0.25-0.625 (suction side) | 0° | 8.5 % | Centerline effectiveness, lateral effectiveness, and effectiveness contours. |
| Balasubram aniyan and Jubran [28] | Numerical/flat plate model. | Single round hole / multiple hole (row of two hole) | 200 µm | 1.75-10 | 0.5 and 1.0 | 35° | 1.0 % | Centerline effectiveness, lateral effectiveness, and flow structure. |
| Ochrymiuk [29] | Numerical/flat plate model. | Multiple holes (112700 hole) | 100 µm diameter | 5 | 1.0 | 30° | - | Film effectiveness |
| Current study | Numerical/flat plate model. | Single round hole | 200 µm | 1.75 | 0.25, 0.5, 1.0 and 1.5 | 35° | 0.2%, 1%, 5%, 10%, and 20% | Centerline effectiveness, lateral effectiveness, and flow structure. |

Based on the above-mentioned literature, it has been found that reducing the cooling hole exit area to a micro-size has shown an improvement in the film cooling performance in contrast to the macro size along with a significant saving in the coolant flow usage. However, most of the previous experimental and numerical studies on the micro hole/slot film cooling were done at limited

blowing ratios at low freestream turbulence intensity. Moreover, because of the substantial influence of the blowing ratio on the thermal and flow field and the interaction of the coolant jet with the freestream, there was no clear description on how the micro hole could affect the flow field whereas one study reported the nonexistence of the vortical structure [30]. Thus, it is necessary to investigate the effect of the blowing ratio on micro hole thermal and flow field as well as the effect of the freestream turbulence intensity. Therefore, the purpose of this numerical study is to investigate the film cooling performance as well as it's thermal and flow field of a single cylindrical micro hole with a 200 µm diameter at a range of blowing ratios M=0.25-1.5. Also, this study investigates for the first time the significate impact of freestream turbulence intensity on micro hole film cooling performance whereas a five FSTI are tested FSTI= 0.2%, 1%, 5%, 10%, and 20% at two blowing ratios M=0.5 and 1.0.

## 1.  Numerical Considerations

### 1.1. Geometry and Simulation Parameters

The geometry investigated in this study for the single cylindrical micro hole was duplicated from the benchmark study of  Sinha et al.  [31] that used to validate the current numerical results. However, the reference hole diameter herein is the diameter of the circular micro hole Dm=200 µm. Also the model is identical to the micro hole computational model in the study of Balasubramaniyan and Jubran [28], but the only difference is the location of the origin point in which in their research they located it at the center of the cooling hole, however, in the present study, it is located at the hole trailing edge to mimic the same model of [31]. The cooling hole has L/D =1.75, P/D = 3, and injected at α= 35°. The freestream channel is extended 10 D above the plate surface, and a plenum is included with a dimension of (8D, 4D, and 3D) in (X, Y, and Z), respectively. The computational model is extended 30D downstream the hole trailing edge and 19D upstream the hole leading edge. The details of the 3D geometry are shown in Fig. 1 a). It is crucial to mention here that benchmark study of  Sinha et al. [31] is chosen for validating the numerical results because of the following reasons: (1) the experimental setup used a flat plate model made from polystyrene foam with very low thermal conductivity (0.027 W/m.K) which significantly eliminated the conduction error, (2) in the experiment a short round cooling hole feed by plenum is used, which is a real representation of turbine blades, and (3) the experiment measurements uncertainty were (±1.0 %),  (±0.7 %), and (±0.5 %) for freestream velocity, total mass flow rate of the jet, and density ratio, respectively. Thus, it is commonly believed that this experimental is one of the most accurate measurements of film cooling distribution of cylindrical hole, and is widely used for validation in many of previous numerical studies [32].

The boundary conditions applied to the computational model are also matching the experimental setup of Sinha et al. [31] for the freestream and the coolant, as shown in Table 2. The temperature of the freestream at the freestream inlet is = 300 K, and the temperature of the coolant is = 150 K at the plenum inlet, which maintains the flow at a density ratio of two (D.R=2). The turbulent parameters include turbulent intensity of freestream (FSTI) = 0.2% and the plenum turbulent intensity = 2.0%, and the viscosity ratios ($\mu_t/\mu$) = 30 % for the plenum  and 50 % for the freestream [33].  The blowing ratios investigated are M= 0.25, 0.5, 1.0, and 1.5. The details of the boundary conditions applied to the model are shown in Fig. 1 b). Noting that the blowing ratio is defined as ( M= D.R *($V_c/V_\infty$), whereas ($V_c/V_\infty$) is the velocity ratio between the coolant and the mainstream. Thus, to get the required blowing ratio, the freestream velocity is kept constant at 20 m/sec at the freestream inlet while the coolant velocity is changed at the plenum inlet. Table 3 demonstrates the calculated coolant velocity at the plenum inlet at various blowing ratios. For the cases that

studied the effect of the freestream turbulence intensity on the micro hole cooling performance, in addition to the previous values, (FSTI= 1%, 5%, 10%, and 20%) are also simulated at two blowing ratios M=0.5 and 1.0.



(a) The computational domain and its dimensions.      (b) The model applied boundary conditions.
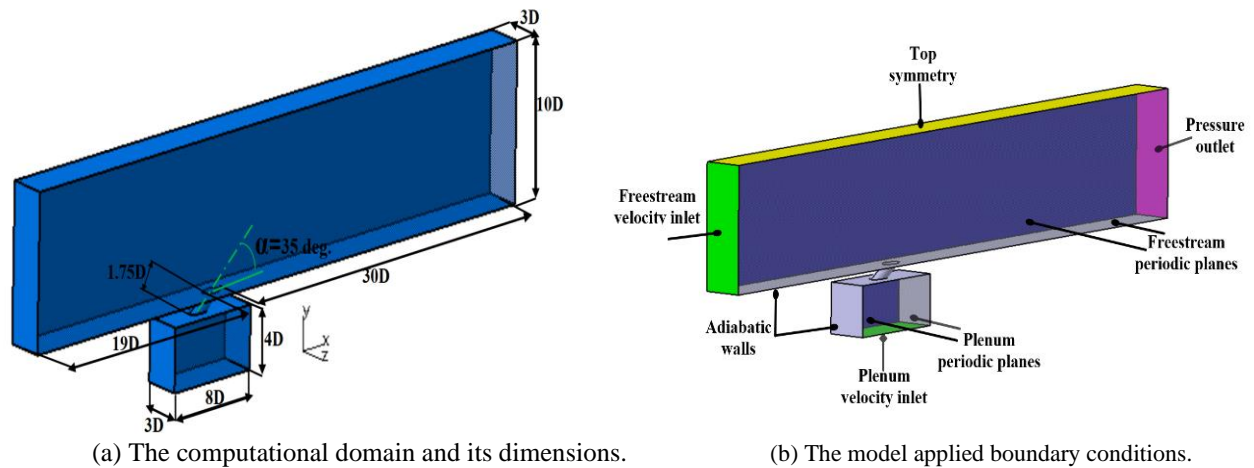
Figure 1. The 3D computational domain dimensions and the applied boundary conditions.

Table 2. The mainstream and coolant flow parameters.

| Property | Value/units |
|---|---|
| Coolant temperature | 150 (K) |
| Freestream velocity | 20 (M/SEC) |
| Freestream temperature | 300 (K) |
| Density ratio (D.R) | 2 |
| Operating pressure | 101.325 (KPA) |

Table 3: The coolant velocity at the plenum inlet.

| M | Coolant velocity Vc (m/sec) |
|---|---|
| 0.25 | 0.082 |
| 0.5 | 0.164 |
| 1 | 0.327 |
| 1.5 | 0.491 |

## 1.2. Mathematical Modelling

The governing equations that used to define the thermal and flow fields in the current numerical assessment of micro hole film cooling are the Reynolds Averaged Navier Stokes (RANS) equations that consist of the continuity equation, momentum equation, and energy equation, which are written in equations. (1) to (3).

$$\frac{\partial U_i}{\partial X_i} = 0 \tag{1}$$

$$\rho U_i \frac{\partial U_j}{\partial X_i} = -\frac{\partial p}{\partial X_j} + \mu \frac{\partial^2 U_j}{\partial X_i \partial X_i} - \frac{\partial}{(\partial X_i)}(\rho \overline{u_i u_j}) \tag{2}$$

$$U_i \frac{\partial \Theta}{\partial X_i} = \alpha \frac{\partial^2 \Theta}{\partial X_i \partial X_i} - \frac{\partial}{\partial X_i}(\overline{u_i \theta}) \tag{3}$$

Whereby the term $(\rho \overline{u_i u_j})$ in Eq. (2) is the Reynolds stress tensor while the term $(\overline{u_i \theta})$ in Eq. (3) is the turbulent heat flux, which yield a closure problem for this system of the equations. Thus, to solve this problem, the tuebulence stress tensor and the turbulent heat flux need to be modelled through turbulence models. The detailed description of the modelling of the Reynolds stress tensor and the turbulent heat flux along with the relizable k-epsilon turbulence model are given in Ref. [34] and [35].

## 1.3. The Mesh and Computational Overview

The mesh of the micro hole computational model was done on ANSYS ICEM 17.1 meshing tool with the aid of the hexahedral unstructured mesh feature. The hexahedral cells were selected for the entire domain, and O-grid cells are wrapped around the cooling hole, as shown in Figure 2. Furthermore, the generated mesh was very fine near the wall and close to the hole region to maintain y+ value less than one at all locations and to ensure that the viscous sublayer is resolved. The cooling performance will be evaluated in terms of adiabatic film cooling effectiveness that includes both centerlines and laterally averaged film cooling effectiveness, as shown in equations (4) and (5), respectively.

$$\eta_c = \frac{T\infty - T_{aw}}{T\infty - T_c} \tag{4}$$

$$\bar{\eta} = \frac{1}{l} \int_0^l \eta dz \tag{5}$$

Whereas $T_\infty$, $T_{aw}$, and $T_c$ are the temperature of the freestream, the adiabatic wall temperature, and temperature of the coolant, respectively. (l) is the length of the lateral distance in the spanwise direction.
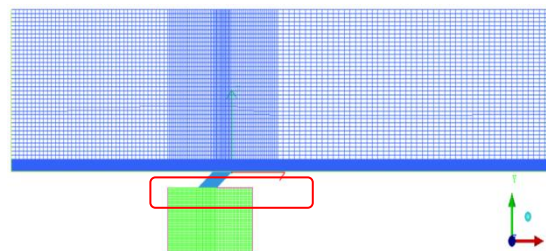


(a) A front view of the mesh.
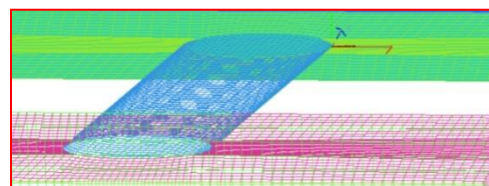


(b) The mesh generated for the cooling hole vicinity region.

Figure 2. The computational domain generated grids for the micro round hole.

The micro hole film cooling simulation was performed using ANSYS Fluent 17.1 package as steady-state analysis. The solution method for the RANS equations was based on the second-order upwind scheme, while the SIMPLEC discretized scheme was used to solve the velocity-pressure coupling for the incompressible ideal flow. The realizable k-ε (RKE) was selected as a turbulence model with enhanced wall treatment (EWT) for near-wall modelling. The simulation cases were considered reached conversion when the residuals for the continuity equation and all velocity components reached ($1\times10^{-4}$), and the energy equation residuals reached ($1\times10^{-6}$). It should be mentioned here that for consistency and comparison purpose, the macro round cooling hole computational model used for validation of the present numerical result is similar to the experimental model of [31] with a hole diameter ($D_M$=12.7 mm). Furthermore, a similar procedure is applied to generate the mesh and numerical setup that stated above for the micro hole case. Note that, primary results of the present investigation are presented by Abd Alsalam and Jubran [36].

## 2.   Results and Discussion

### 2.1. Sensitivity Analysis

Mesh sensitivity analysis is performed at a blowing ratio of M=1.0 for the centerline film cooling effectiveness, as shown in figure 3, whereas the numerical results are compared with the experimental data of [31]. The macro hole mesh independency study carried out for four different meshes and fine mesh (1) with $1.45\times10^6$ cells are satisfying the mesh sensitivity, and it is going to be used to carry further the second stage of macro hole film cooling performance validation. The second stage of the validation of the present numerical results is used to examine the selected fine mesh (1) to predict both the centerline and the laterally averaged film cooling effectiveness at low and high blowing ratios M=0.5 and 1.0 that shown in Figures 4 and 5, a) and b), respectively. The simulation results of the macro hole centerline and the laterally averaged film cooling effectiveness presented in Fig. 4 a) and b) at blowing ratio M=0.5, generally illustrate a good agreement in capturing the cooling effectiveness compared with the experimental data of [31]. However, there is a little bit of overprediction of the centerline performance in the downstream region of the cooling hole at (X/D < 10). The results of the high blowing ratio case M=1.0, shown in Fig 5 a) and b), present reasonable prediction of the centerline and laterally averaged film cooling effectiveness using the realizable k-ε turbulence model with the enhanced wall treatment as well as it captures the separation and reattachment region at ( $2\leqslant X/D \leqslant 5$), shown in figure 5 a). Also, there is a slight overprediction of the centerline effectiveness for the whole downstream region of the cooling hole and a slight underprediction of the spreading of the coolant in the spanwise direction compared to the experimental data. This overprediction of the numerical results comes as a result of the isotropic feature of the k-ε turbulence model, as reported in [30,31]. It can be roughly said that the numerical results are relatively precise and reliable as well as they show the capability of the RKE turbulence model with EWT in capturing the cooling performance. Similarly, the mesh sensitivity of a 200 μm diameter discrete cylindrical micro hole is performed and obtained at about $1.39\times10^6$ cells.

### 2.2. Effectiveness Results of the Micro Hole with the Effect of Blowing Ratios

The numerical results of the centerline and laterally averaged film cooling effectiveness of the cylindrical micro hole with the influence of the blowing ratio are presented in Figure 6 a) and b), respectively. It can be seen from Fig. 6 a) that all blowing ratios have shown high centerline effectiveness, which is close to unity right away at the hole exit. By comparing the micro hole centerline effectiveness results to that of the macro hole, the centerline effectiveness is almost the

same for both holes. However, it drops immediately further downstream at (X/D >1) whereas different behaviour has been observed by increasing the blowing ratio. The rate of the decline of the centerline cooling effectiveness for the micro hole cases is higher than that for the macro hole. The reason for that could be due to low microjet momentum whereas the ejected coolant gets rapidly mixed with the freestream and caused a reduction in the ability of the microjet to maintain its structure specifically in the hole vicinity region. The low blowing ratios cases M=0.25 and 0.5 reveal approximately similar centerline cooling performance and consistent profile, which become flattened in the downstream region at (X/D ≤ 20).
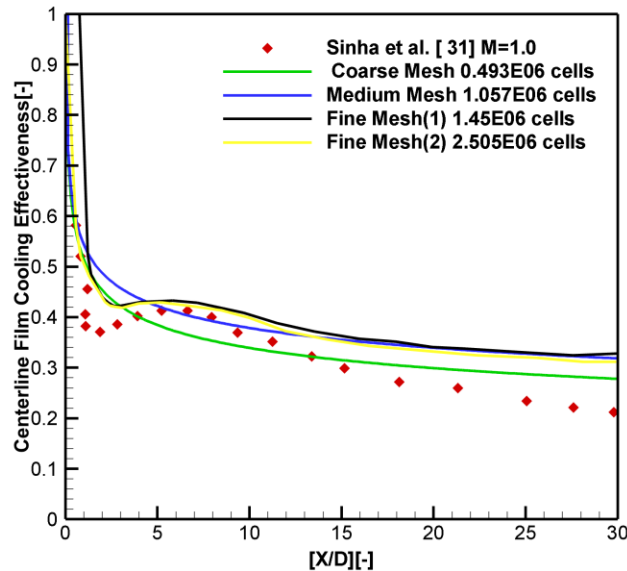


Figure 3. The mesh sensitivity for the macro hole shows the centerline film cooling effectiveness at M=1.0.



(a) The centerline film cooling effectiveness.

(b) The laterally averaged film cooling effectiveness.
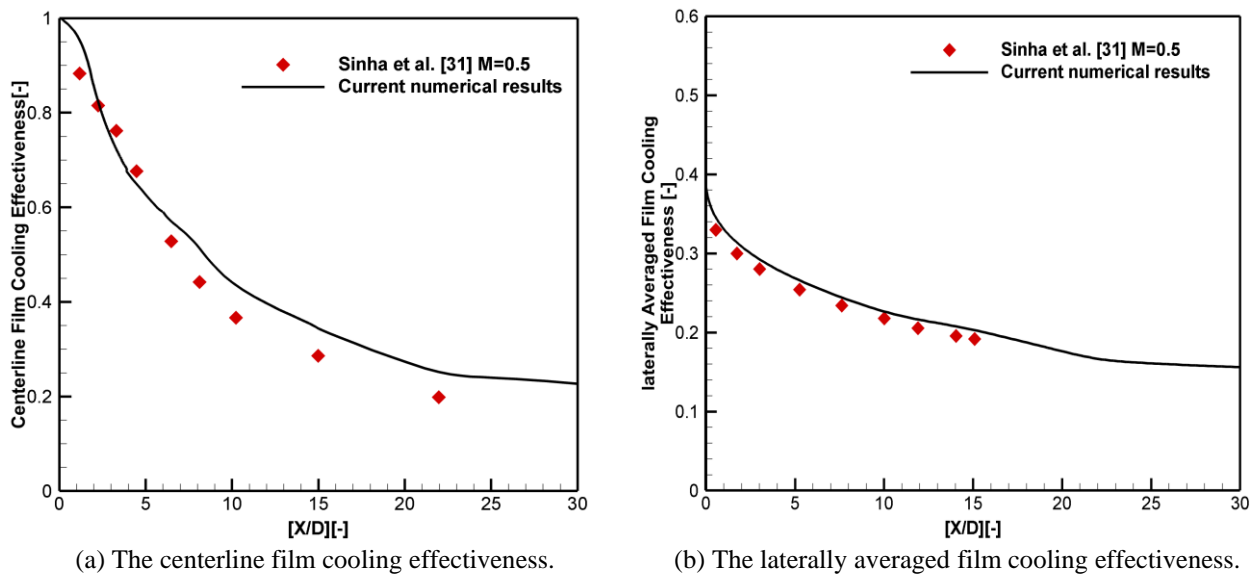
Figure 4. The macro hole centerline and laterally averaged film cooling effectiveness at M=0.5 and D.R=2 compared with the experimental data of [31].

(a) The centerline film cooling effectiveness.      (b) The laterally averaged film cooling effectiveness.
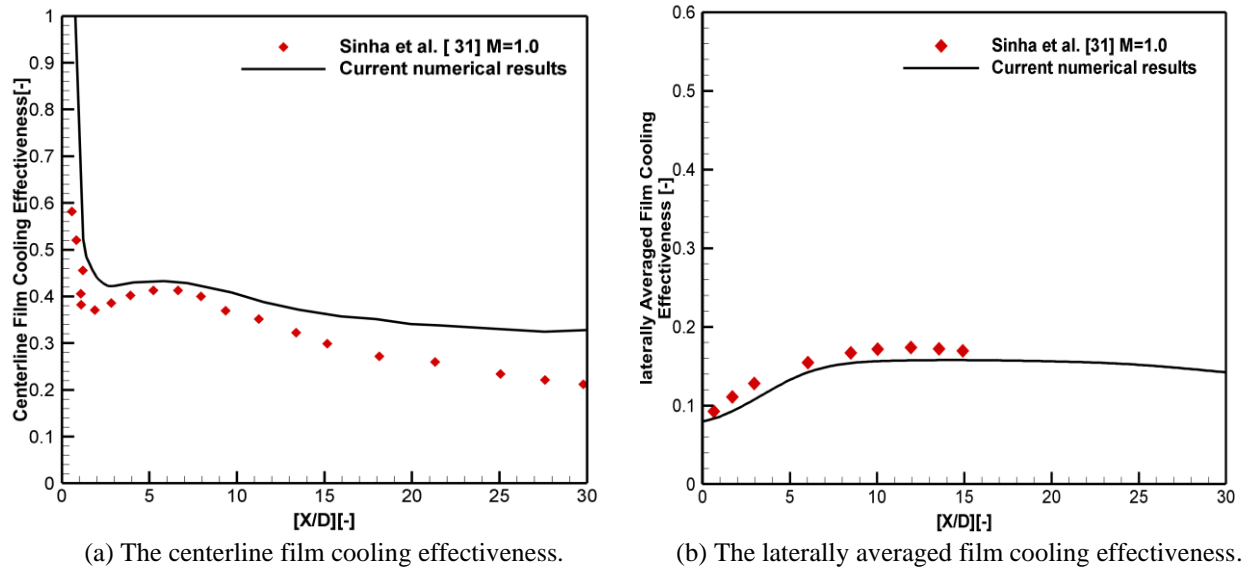
Figure 5.The macro hole centerline and laterally averaged film cooling effectiveness at M=1.0 and D.R=2 compared with the experimental data of [31].

Interestingly, the blowing ratio M=0.25 has shown the optimum centerline performance, and it is only about 5 % higher than that attained at blowing ratio M=0.5. This may give a good chance for the flexibility of protecting the turbine blades during operation within this range of blowing ratios while achieving a good engine performance with less coolant consumption. In contrast to the micro hole, the macro hole film cooling optimum performance was attained at blowing ratio M=0.5 as reported in most of the literature. The centerline film effectiveness results at high blowing ratios are also presented in Figure 6 a). As expected, increasing the blowing ratio from 1.0 to 1.5 leads to a faster decay in the centerline effectiveness and as a result of increasing the microjet coolant momentum, the coolant jet lift-off phenomenon occurs and causes a separation of the coolant jet from the plate surface. However, further downstream at $(X/D \geq 20)$, due to the reattachment of the coolant jet, the centerline effectiveness restores its performance to provide the highest centerline effectiveness which is even above the one obtained at M=0.25. Comparing the micro hole cooling performance of the current study to the previous numerical results of Balasubramaniyan and Jubran [28], there is a good agreement between both results at blowing ratio M=0.5 and 1.0 in the far downstream. But in the hole vicinity region, a slight divergence is noticed whereas Balasubramaniyan and Jubran have found that the micro hole performs somewhat better than the macro hole at $(X/D \leq 1.0)$ which is not the case in the current study. This might be due to the difference in the applied turbulence boundary conditions that are resulting in a different prediction for flow field results in the hole vicinity region.

The micro hole laterally averaged film cooling effectiveness results with the effect of the blowing ratio are shown in Figure 6 b). Generally, the laterally averaged effectiveness performance of the micro hole is better than that of the macro hole in the hole vicinity region at $(X/D \leq 5.0 )$ for all blowing ratios, while both holes have shown similar performance far downstream at high blowing ratios. It is also found that the coolant jet at low blowing ratios spreads more widely in the lateral direction in the adjacent downstream region of the hole up to $(X/D \leqslant 5.0)$, while far downstream, the high blowing ratios show better diffusion of the coolant. The optimum laterally averaged film cooling effectiveness is found at low blowing ratio M= 0.5 at $(X/D \leq 5.0)$, while in the far

downstream area the best performance is obtained by blowing ratio of M=1.5. The good lateral performance of the micro hole at M=0.5 could be attributed to the characteristic of the microjet in which it has a less turbulent enhancement and penetration into the mainstream as pointed out by Hassan [39]. Furthermore, the other most likely reasons for this good performance are that the micro coolant jet had shown a better local lateral performance at low and high blowing ratios (M=0.5 and 1.0) as reported in ref. [28], and the 3D flow structure of the microjet that showed a reduction in the strength and size of the CRVP, which will be shown next in the results.



(a) The centerline effectiveness.       (b) The laterally averaged effectiveness.
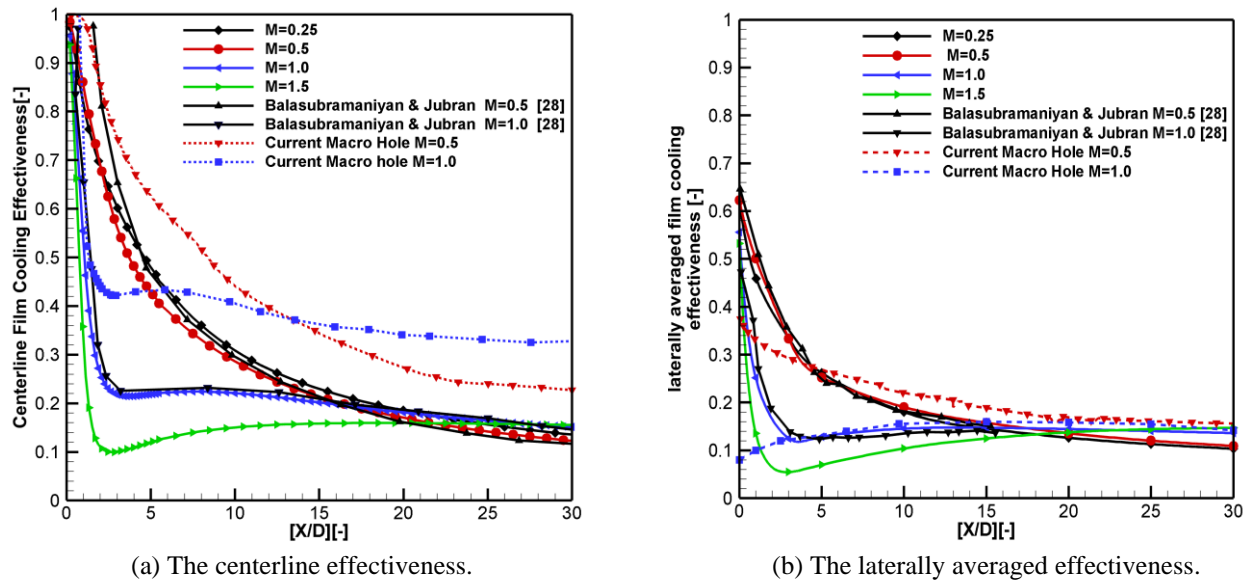
Figure 6. The micro hole centerline and laterally averaged film cooling effectiveness M=0.25-1.5.

To present the expected benefits that could be attained from the cylindrical micro hole in terms of the improvement in the cooling performance, a comparison is performed between the overall averaged film cooling effectiveness for a discrete micro and macro hole as a function of blowing ratio, and the results are shown in Figure 7. The plot apparently shows that the micro hole overall averaged film cooling effectiveness is higher than that from the macro hole by approximately 30 %. To exhibit how much the micro cooling is assisting the coolant distribution in the lateral direction, which is one of the leading problems in the cylindrical macro hole, a comparison is performed for micro and macro holes laterally averaged effectiveness results as a function of the blowing ratio, as shown in Figure 8 whereas interesting results are found for blowing ratios of M=0.25 -1.5. It can be said that the micro hole in most of the examined blowing ratios cases show a higher average laterally averaged effectiveness because of the improvement in the spanwise coolant diffusion and being more uniform. However, it shows a slightly lower performance at M=0.5, and the reason for this could be that the coolant jet is not capable of maintaining its structure due to mixing and thus resulting in a reduction in the cooling performance. Also, it can be depicted from the same plot that the micro hole has accomplished this good lateral performance with about 12 % reduction in the coolant blowing ratio at the range of the highest averaged lateral film cooling effectiveness, indicating a reduction in coolant consumptions. So, this progression in the micro hole film cooling effectiveness increases the potential of applying this micro-cooling technology as an effective method to cool turbine blades.
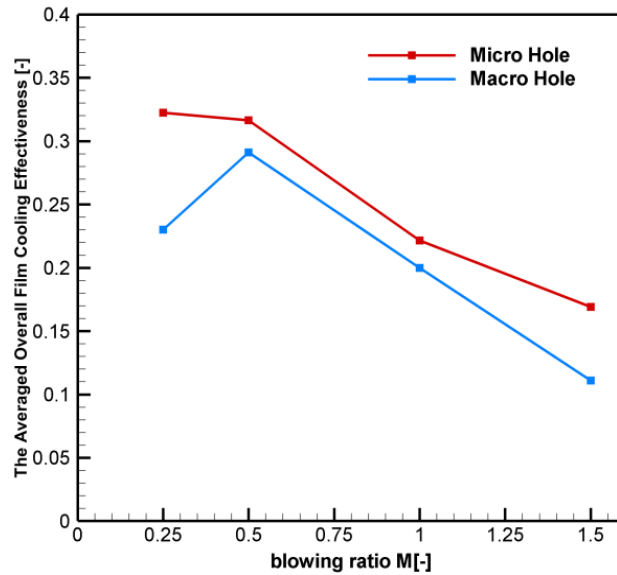
Figure 7. The comparison of the average overall film cooling effectiveness versus the blowing ratio for the macro and micro cylindrical cooling hole.
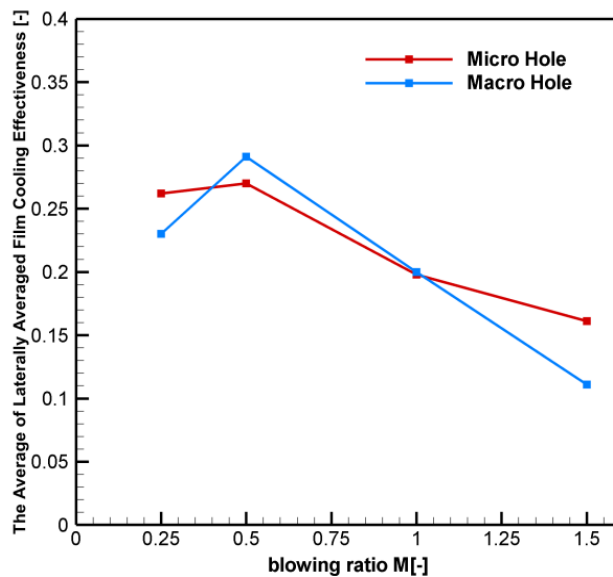


Figure 8. The comparison of the average of laterally averaged film cooling effectiveness versus the blowing ratio for the macro and micro cylindrical cooling hole.

## 2.3. Flow Field Results

In this section, the impact of the micro hole film cooling technique on the surrounding flow field is presented in terms of the velocity field and flow structure. The analysis of the velocity contours is exhibited at the midplane z=0 at four blowing ratios while the emphasis is mainly in the hole vicinity region, as shown in Fig. 9. The velocity contours at low blowing ratios M= 0.25 and 0.5, shown in Fig. 9 a) and b), illustrate a highly skewed jet inside the cooling hole turned toward the hole leading edge which leads to a low jet momentum at the hole trailing edge. Consequently, at the moment of the interaction of the mainstream with the coolant, the mainstream will force the coolant to remain attached to the plate surface, which explains why micro hole has a good cooling

performance at low blowing ratios M=0.25 and 0.5. For the case of M=1.0, shown in Figure 9 c), the velocity contour displays a wider reverse region downstream the hole exit along with a high jet momentum at the hole leading edge. As such, the jet lifted off from the plate surface and caused a reduction in the centerline and laterally averaged film cooling effectiveness. For the highest blowing ratio case M=1.5, shown in Figure 9 d), it can be seen that the microjet has a very high coolant momentum inside the cooling hole that leads to coolant jet lift-off from the surface and then reattach to it further downstream. Accordingly, the cooling performance of the micro hole immediately drops in the hole adjacent region at ($1 \leq X/D \leq 4$) as shown early in Fig 6 a). In general, the influence of the blowing ratio on the flow field of a single micro hole has shown a similar trend to that of the macro hole in which the coolant flow jet either remain attached, lifted off, or reattached to the plate surface based on the blowing ratio, which was reported in many of the previous CFD and experimental studies [31],[32],[37], [40], and [41].
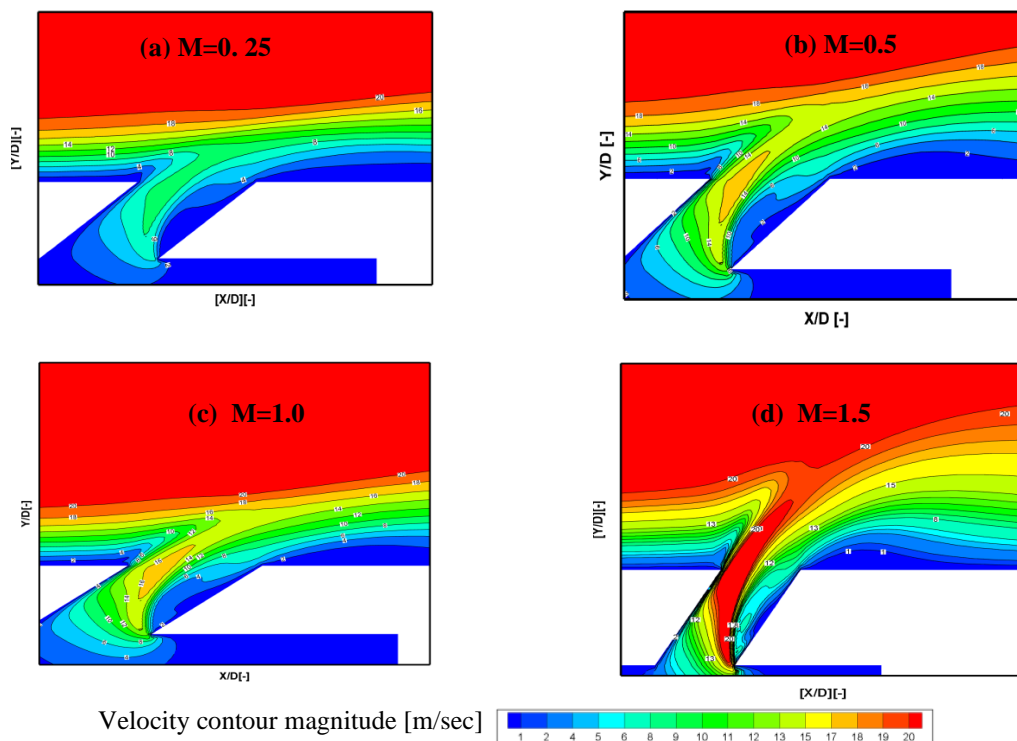


Figure 9. The velocity contour at midplane z= 0 at blowing ratio M=0.25-1.5.

The 3-D complex flow structure generated from the interaction of the freestream with the coolant jet that primarily exhibited in the counter-rotating vortices pair (CRVP) which has a significant effect on the cooling performance and contributed to jet lift-off phenomenon. As such, a comparison of the flow structure is carried out herein first between the macro and micro-holes at blowing ratio of M=0.5 for four locations downstream of the hole; X/D= 0, 1, 3, and 5. Second, the flow structure is also investigated for the micro hole at various blowing ratios M=0.25 to 1.5. The flow structure results are shown in YZ plane with the aid of the velocity vector combined with the temperature contours in which the velocity vector will be used to indicate the vortices strength and size, while the temperature contour will show the mixing rate of the coolant with the mainstream. Figure10 a) and b) shows the flow structure results at M=0.5 for macro and micro holes, and it can be seen that the coolant core is notably attached to the plate surface for both holes

|  X/D=0 | X/D=1 | X/D=3 | X/D=5 |

(a) Macro hole M=0.5

(b) Micro hole M=0.5

(c) Micro hole M=0.25

(d) Micro hole M=1.0

(e) Micro hole M=1.5

Temperature [K]

150 160 170 180 190 200 210 220 230 240 250 260 270 280 290 300
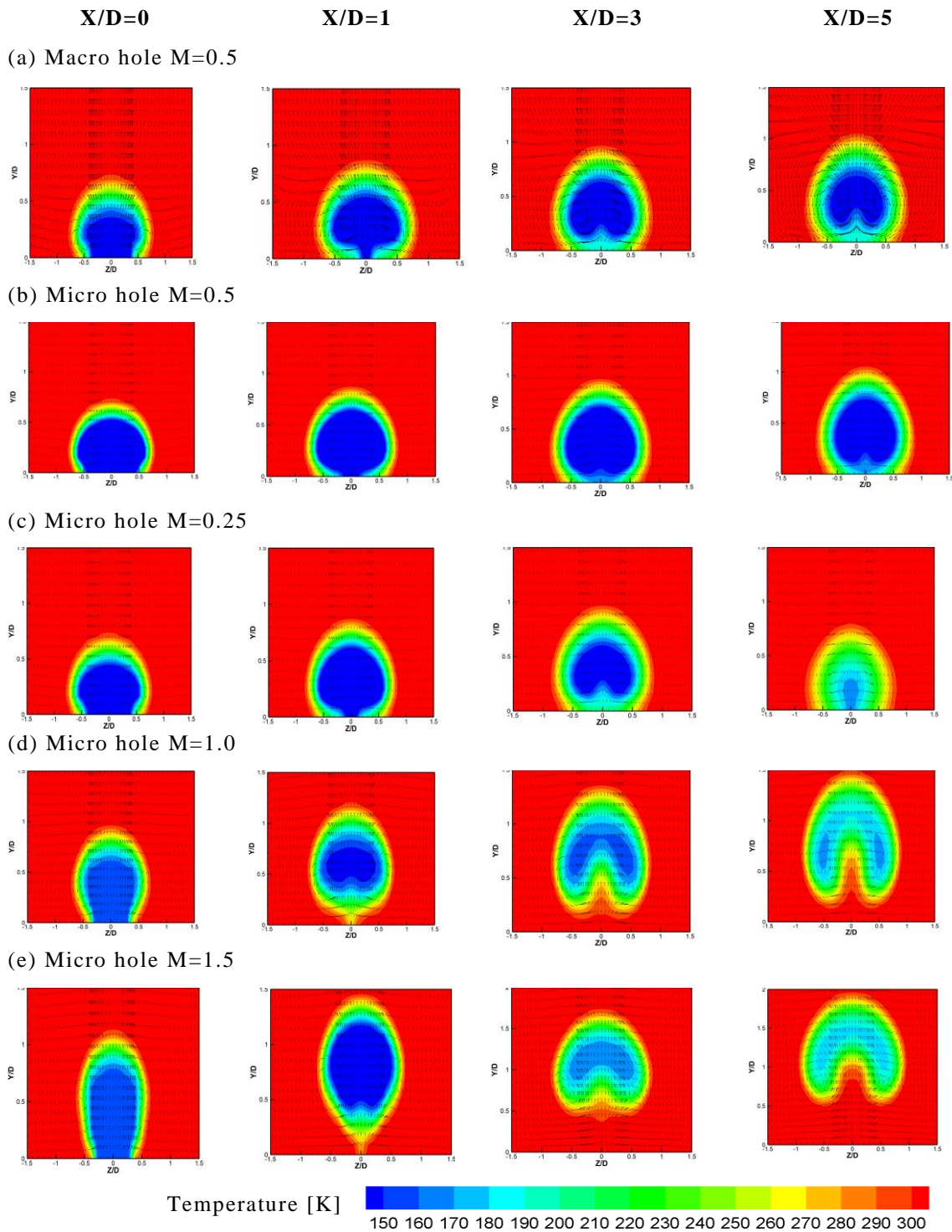
Figure 10. The flow structure results at four different locations downstream of the cooling hole at X/D=0, 1, 3, and 5 at various blowing rate M=0.25 – 1.5.

at the downstream locations of (X/D= 0 and 1). Also, the core attachment region of the micro hole is much wider than that of macro hole whereas the coolant core at (X/D=0) covers the lateral domain of (±0.4) and (±0.5) for the macro and micro holes, correspondingly, while at (X/D=1) it

covers the domain of (±0.15) and (±0.3), for the macro and micro holes, correspondingly. The vertical coolant distribution of the micro and macro hole is almost identical. Moreover, the mixing of coolant and freestream from the micro hole is less than that of the macro hole, and the coolant core is more competed for the macro hole, as depicted by temperature contours. In terms of the vortices structure, Figure 10 a) and b) illustrate the deformation of stronger counter-rotating vorticity pair structure, which attempts to lift the coolant away from the surface in the case of the macro hole. Instead, the micro hole has waker and less defined vortices structure, which reduces the mixing of coolant with the mainstream, and this enhances the coolant spreading in the spanwise direction. Moving further downstream, at (X/D=3 and 5), the coolant core is still attached for the macro and micro hole at those two positions, but the micro hole still shows a wider coolant distribution spanwisely whereas at (X/D=3) the coolant covers the lateral region of (±0.135) for the macro hole, and it covers the area of (±0.28) for the micro hole. While at (X/D=5) the coolant covers the region of (±0.12) and (±0.25) for the macro and micro holes, respectively. Also, because of the devolvement of the CRVP and its stronger structure, it enhances the mixing, and it reduces the coolant lateral distribute compared to that of the micro hole. On the other hand, the swirling flow starts to be less notable from the micro hole, and the CRVP is very weak. The flow structure for the lowest blowing ratio case of the micro hole, M=0.25, shown in Figure 10 c) displays the coolant jet is attached to the plate surface in the hole vicinity area at (X/D = 0 and 1), while the coolant lateral coverage is slightly less than that of the micro hole at M=0.5. Further downstream at (X/D= 3 and 5), the coolant jet could not hold its structure, and it gets mixed rapidly with the freestream as a result of low coolant jet momentum while a less define CRVP has appeared.

The adverse effect of the CRVP is more distinct on the micro hole cooling performance in the hole adjacent area at high blowing ratio, as shown in the case of M=1.0 Figure 10 d) and M=1.5 Figure 10 e). In those two cases, the coolant core is shown only to be attached to the surface at (X/D= 0) while the coolant has a high jet momentum that causes the jet to lift-off from the plate surface while intense mixing occurs. As such, micro hole cooling performance is degraded in the downstream region ( 1< X/D<5) at high blowing ratios.

## 2.4. Freestream Turbulence Intensity Effect on Film Cooling

The numerical results of micro hole film cooling effectiveness that show the effect of the freestream turbulence intensity on the cooling performance are presented at two blowing ratios M=0.5 and M=1.0. First, quantitatively in terms of the centerline and lateral effectiveness that will indicate how the micro hole will perform under engine like freestream condition. Second, qualitatively by analyzing the local film cooling on the plate surface to exhibit the coolant coverage on the plate surface. The results of the adiabatic centerline film cooling effectiveness of a cylindrical micro hole with the effect of the freestream turbulence intensity at M=0.5 and 1.0 are shown in Figure 11 a) and b), respectively. Ultimately, Fig 11 a) and b) show a similar trend for centerline film cooling effectiveness that displayed early in Fig 6 a), but increasing the freestream turbulence intensity causes a little bit reduction in the performance. The low blowing ratio case M=0.5, shown in Fig 11 a), for various FSTI illustrate that increasing the freestream turbulence intensity from FSTI=0.2% to FSTI=20% has a minor effect on reducing the centerline effectiveness up to downstream distance (X/D ≥ 10) in which the centerline effectiveness is reduced by 4 %. While further downstream the reduction on the centerline performance is a bit higher, whereas the case of FSTI=20 % has the lowest effectiveness, which is about 6 % lower than that at FSTI=0.2 %. This degradation of the centerline film cooling performance comes as a result of enhancing the mixing between the freestream and the coolant jet at high FSTI, and it

seems that the coolant jet was totally dissipated and dispersed at the hole downstream region of $(X/D \geq 20)$. The  centerline effectiveness results at high blowing ratio M=1.0, shown in Fig 11 b), depict that by increasing the  FSTI: (1) a continuation in decline in the effectiveness in the hole vicinity region and far downstream, (2) the separation and the reattachment region is shifted downstream in most of the cases as a result of the intensive mixing between the coolant and the freestream at this high blowing ratio case.



(a) Centerline film cooling effectiveness at M=0.5.          (b) Centerline film cooling effectiveness at M=1.0.
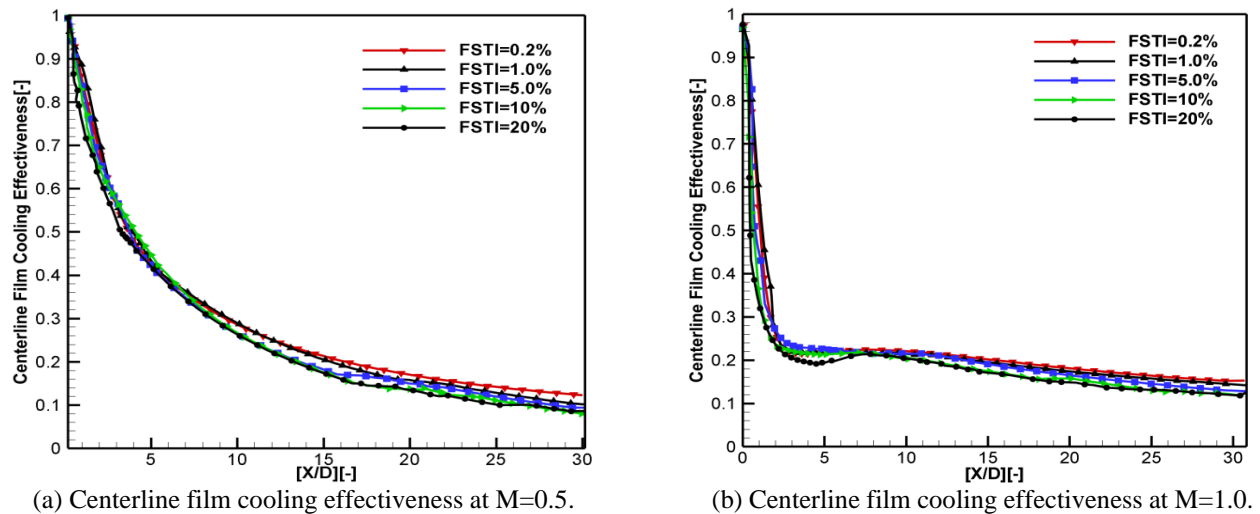
Figure 11. The micro hole centerline film cooling effectiveness at various freestream cooling effectiveness at two blowing ratio M=0.5 and 1.0.

The laterally averaged adiabatic film cooling effectiveness results for the cylindrical micro hole with the influence of the freestream turbulence intensity at low and high blowing ratios M=0.5, and 1.0 are shown in Figure 12 a) and b), respectively.  Fig 12 a) and b) mainly presented the same tendency for the lateral effectiveness performance discussed previously in Fig 6 b, however, increasing the FSTI appears to significantly change the lateral cooling performance. The low blowing ratio cases are shown in 12 a) display an increase in the lateral performance, which is mostly occurred in the downstream region of the cooling hole between $(5 \leq X/D \leq 15)$. The high blowing ratio cases shown in 12 b) exhibit that the lateral effectiveness is improved for the entire downstream region of the cooling hole. Furthermore, Fig 12 b) indicates that increasing the FSTI has affected the location of the separation and the reattachment region wherein it seems to be shifted a bit upstream compared to the case of the lowest FSTI=0.2%. The lateral effectiveness has a higher performance in the case of FSTI = 20% compared to that at FSTI = 0.2%; Which is increased by about 5% and 15 % at blowing ratios M=0.5 and 1.0, respectively. A possible reason for this increase in micro hole lateral cooling performance is because of that increase turbulence intensity caused an increase in the mixing rate between the coolant jet and the freestream which in turn helps to distribute the coolant jet more widely in the spanwise direction.

Figure 13 shows a 2-D contour plot on the plate surface for the local film cooling effectiveness to represent the influence of the freestream turbulence intensity on micro hole cooling performance and to indicate the micro hole coolant coverage. It is clearly presented in Fig. 13 that the zone of the high local film cooling effectiveness appears in the vicinity region of the hole exit for both examined blowing ratios at all levels of freestream intensity whereas the optimum coverage is found at the blowing ratio M= 0.5 and FSTI=20%. Furthermore,  At M=0.5 increasing the FSTI

helps to improve the coolant coverage up to a downstream distance ($X/D \leq 15$), however, further downstream it shows a little bit of reduction in coolant performance due to coolant mixing and dispersion into the freestream. Also, Fig. 13 a) and b) show that the distribution of the local effectiveness for both blowing ratios are symmetrical about the centerline $Z = 0$. The high blowing ratio M= 1.0 shows lower performance compared to that attained at M=0.5 while a wider zone of coolant distribution spanwisely occurs far downstream which reflects the better performance for the micro hole at high blowing ratios in which the coolant coverage improves by increasing the FSTI. This wide distribution of the coolant in the spanwise direction comes as a result of the reattachment of the coolant jet far downstream of the hole exit at high blowing ratio.



(a) Laterally averaged effectiveness at M=0.5.          (b) Laterally averaged effectiveness at M=1.0.
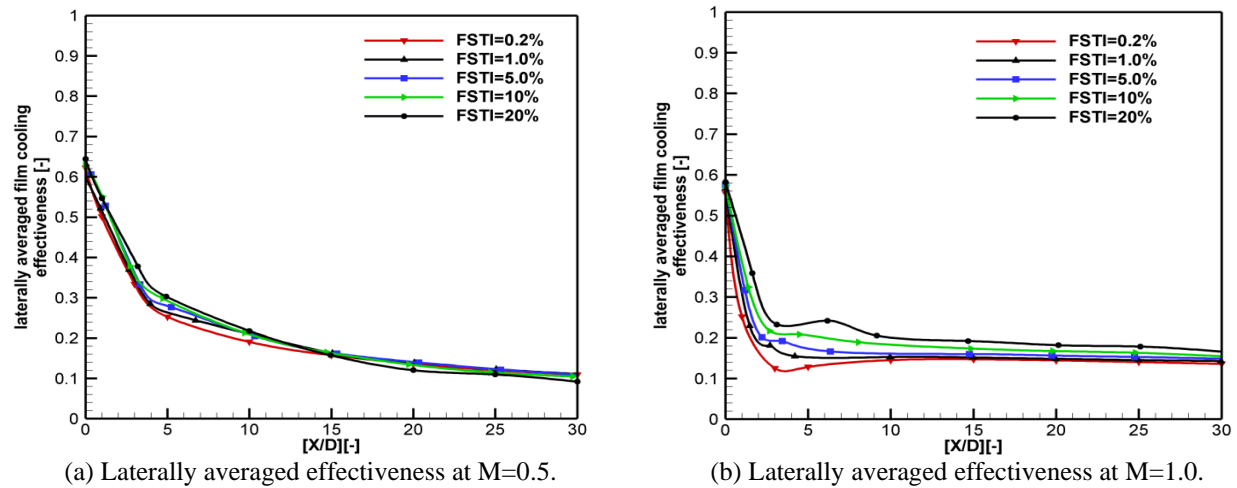
Figure 7. The micro hole laterally averaged film cooling effectiveness at various freestream cooling effectiveness at two blowing ratio M=0.5 and 1.0.



(a) At low blowing ratio M=0.5          (b) At high blowing ratio M=1.0
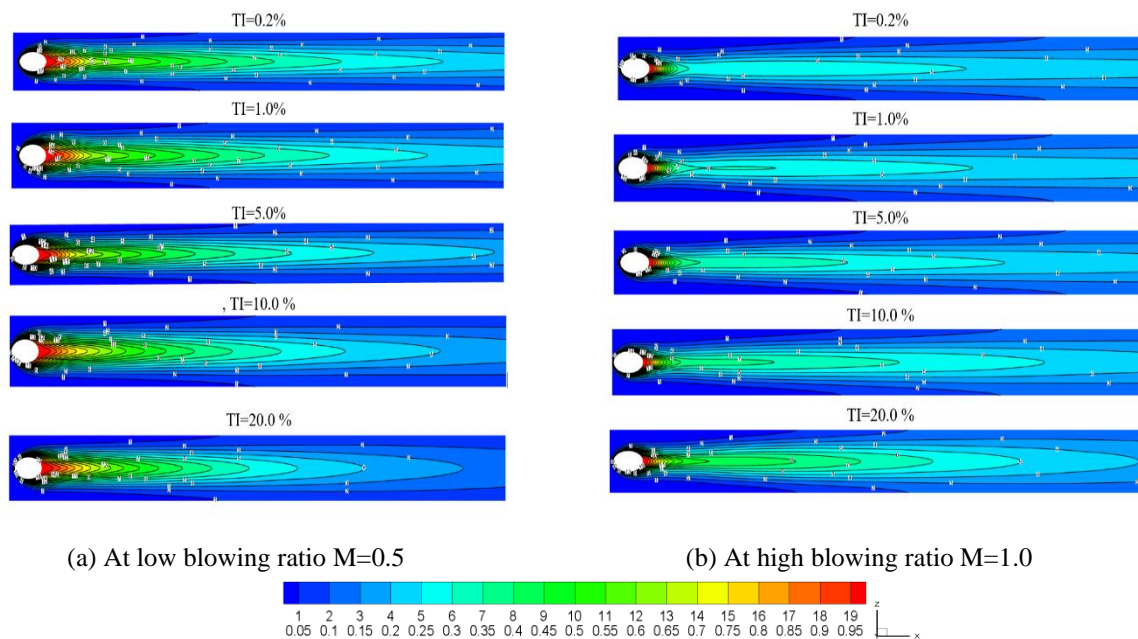
Figure 8. The local film cooling effectiveness contours at the plate surface at various freestream turbulence intensity at blowing ratio M=0.5 and M=1.0.

## 4. Conclusions

This paper has shown that using the CFD simulation; it is possible to predict the cooling performance of a discrete micro film cooling hole with 200 µm diameter on a flat plate, which is very difficult to obtain experimentally under real engine operating conditions as pointed out by Ochrymiuk [29]. It is found that the micro cooling hole produces the best centerline and lateral performance at low blowing ratios. Furthermore, it is found that there is about a 12% reduction in the coolant blowing ratio within the range of the highest averaged lateral effectiveness for the micro hole cases which means a decrease in coolant consumption. The flow field results demonstrate a decrease in the CRVP size and strength, which helps in distributing the coolant more widely in the spanwise direction. At the same blowing ratio, increasing the freestream turbulence intensity to match the engine like operating conditions slightly reduced the centerline effectiveness and caused an increase in the laterally averaged effectiveness. Finally, there is a considerable improvement in the overall film cooling performance that is nearly 30 % higher than that of the macro hole. The micro-cooling technique has the potential to effectively prevent the thermal failure of turbine blade while maintaining its structure and material strength, which leads to more efficient and environmentally friendly aero engines.

## References

[1]     J.-C. Han, S. Dutta, and S. Ekkad, Gas Turbine Engine heat transfer and cooling Technology, 2nd ed. London NewYork: CRC Press, 2012.

[2]     J.-C. Han, "Fundamental Gas Turbine Heat Transfer," J. Therm. Sci. Eng. Appl., vol. 5(2), pp. 021007-021007–15, 2013.

[3]     R. J. Goldstein, "Film Cooling," Adv. Heat Transf., vol. 7, pp. 321–379, 1971.

[4]     K. Javadi, "Introducing Film Cooling Uniformity Coefficient," Heat Transf. Eng., vol. 39(2), pp. 180–193, 2018.

[5]     R. S. Bunker, "Turbine cooling design analysis," in Gas Turbine Handbook - NETL, pp. 295–309, 2006.

[6]     T. I.-P. Shih and V. Yang, Turbine aerodynamics, heat transfer, materials, and mechanics. American Institute of Aeronautics and Astronautics, Inc., 2014.

[7]     A. Kohli and D. G. Bogard, "Effects of very high free-stream turbulence on the jet-mainstream interaction in a film cooling flow," J. Turbomach., vol. 120, no. October 1998, pp. 785–790, 1998.

[8]     D. G. Bogard and K. A. Thole, "Gas Turbine Film Cooling," J. Propuls. Power, vol. 22(2), pp. 249–270, 2006.

[9]     S. Acharya and Y. Kanani, "Advances in Film Cooling Heat Transfer," in Advances in Heat Transfer, 1st ed., vol. 49, Elsevier Inc., pp. 91–156, 2017.

[10]    A. Brown and C. L. Saluja, "Film Cooling from a Single Hole and a Row of Holes of Variable Pitch to Diameter Ratio," Int. J. Heat Mass Transf., vol. 22(4), pp. 525–533, 1979.

[11]    G. W. Jumper, W. C. Elrod, and R. W. Rivir, "Film Cooling Effectiveness in High-Turbulence Flow," J. Turbomach., vol. 113(3), pp. 479–483, 1991.

[12]   J. P. Bons, C. D. Macarthur, and R. B. Rivir, "The Effect of High Freestream Turbulence on Film Cooling Effectiveness," J. Turbomach., vol. 118(4), pp. 814–824, 1996.

[13]   S. W. Burd, R. W. Kaszeta, and T. W. Simon, "Measurements in Film Cooling Flows: Hole L/D and Turbulence Intensity Effects," J. Turbomach., vol. 120(4), pp. 791–798, 1998.

[14]   J. E. Mayhew, J. W. Baughn, and A. R. Byerley, "The effect of freestream turbulence on film cooling adiabatic effectiveness," Int. J. Heat Fluid Flow, vol. 24(5), pp. 669–679, 2003.

[15]   L. M. Wright, S. T. McClain, and M. D. Clemenson, "Effect of Freestream Turbulence Intensity on Film Cooling Jet Structure and Surface Effectiveness Using PIV and PSP," J. Turbomach., vol. 133(4), pp. 041023-1-041023–12, 2011.

[16]   C. Saumweber, A. Schulz, and S. Wittig, "Free-Stream Turbulence Effects on Film Cooling With Shaped Holes," J. Turbomach., vol. 125(1), pp. 65–73, 2003.

[17]   D. S. DUVALL, "The Use of Lasers in Gas Turbine Manufacturing," in The American Society of Mechanical Engineers, 1985, pp. 1–7.

[18]   C. A. McNally, J. Folkes, and I. R. Pashby, "Laser drilling of cooling holes in aero-engines: state of the art and future challenges," Mater. Sci. Technol., vol. 20(7), pp. 805–813, 2004.

[19]   M. Tyrrell, "It all adds up for engines – Aerospace Manufacturing Magazin," Aerospace Manufacturing Magazine, 2017.

[20]   G. Cerri, A. Giovannelli, L. Battisti, and R. Fedrizzi, "Advances in effusive cooling techniques of gas turbines," Appl. Therm. Eng., vol. 27(4), pp. 692–698, 2007.

[21]   R. S. Bunker, "Turbine Cooling: Moving From Macro To Micro Cooling," in Proceedings of ASME Turbo Expo 2013: Turbine Technical Conference and Exposition GT2013 GAS, 2013, pp. 1–17.

[22]   AITEB 2 Project, "Aerothermal Investigations on Turbine Endwalls and Blades Project Summary," 2008.

[23]   J. Green, "Micro-Scale Film Cooling for Gas Turbine Applications," MSc Thesis, Aerospace engineering Department, Cranfield University, UK, 2007.

[24]   R. Sriram and G. Jagadeesh, "Film cooling at hypersonic Mach numbers using forward-facing array of micro-jets," Int. J. Heat Mass Transf., vol. 52(15–16), pp. 3654–3664, 2009.

[25]   M. Barzegar Gerdroodbary, M. Imani, and D. D. Ganji, "Investigation of film cooling on nose cone by a forward-facing array of micro-jets in Hypersonic flow," Int. Commun. Heat Mass Transf., vol. 64, pp. 42–49, 2015.

[26]   P. L. Li, H. S. Ko, D. Z. Jeng, C. W. Liu, and C. Gau, "Micro film cooling performance," Int. J. Heat Mass Transf., vol. 52(25–26), pp. 5889–5894, 2009.

[27]   O. Hassan and I. Hassan, "Experimental investigations of the film cooling effectiveness of a micro-tangential-jet scheme on a gas turbine vane," Int. J. Heat Mass Transf., vol. 61(1), pp. 158–171, 2013.

[28]   S. Balasubramaniyan and B. A. Jubran, "Numerical analysis of film cooling from micro-hole," Springer Berlin Heidelberg, 2013.

[29]   T. Ochrymiuk, "Numerical analysis of microholes film/effusion cooling effectiveness," J. Therm. Sci., vol. 26(5), pp. 459–464, 2017.

[30]   H. M. Li and I. Hassan, "The Effects of Counterrotating Vortex Pair Intensity on Film-Cooling Effectiveness," Heat Transf. Eng., vol. 36(16), pp. 1360–1370, 2015.

[31]   A. K. Sinha, D. G. G. Bogard, and M. E. E. Crawford, "Film-cooling effectiveness downstream of

a single row of holes with variable density ratio," J. Turbomach., vol. 113(3), pp. 442–449, 1991.

[32]   X. Z. Zhang and I. Hassan, "Film Cooling Effectiveness for an Advanced-Louver Cooling Scheme for Gas Turbines," J. Thermophys. Heat Transf., vol. 20(4), pp. 754–763, 2006.

[33]   S. Khajehhasani and B. A. Jubran, "A Numerical Evaluation of the Performance of Film Cooling from a Circular Exit Shaped Hole with Sister Holes Influence," Heat Transf. Eng., vol. 37(2), pp. 183–197, 2016.

[34]   ANSYS Inc., ANSYS FLUENT User's Guide, Release 13. Canonsburg, PA, 275 Technology Drive Canonsburg, PA 15317, 2010.

[35]   D. C. Wilcox, Turbulence Modeling for CFD, 3rd ed. DCW Industries Inc., 2006.

[36]   S. Abd Alsalam and B. Jubran, "Numerical Evaluation of Film Cooling Performance of a Cylindrical Micro Hole with the Influence of the Blowing Ratio," in Proceedings of the 26st Annual Conference of CFD Society of Canada, Winnipeg, Manitoba, Canada.,pp. 1–11, 2018.

[37]   P. L. Johnson, V. Shyam, and C. Hah, "Reynolds-Averaged Navier-Stokes Solutions to Flat Plate Film Cooling Scenarios," Natl. Aeronaut. Sp. Adm. Glenn Res. Cent., no. No.Nasa-Tm-217025, pp. 1–12, 2011.

[38]   S. Khajehhasani, "Numerical Modeling of Innovative Film Cooling Hole Schemes," Ph.D. thesis, Aerospace engineering, Ryerson University, 2014.

[39]   O. Hassan, "Thermal and Flow Field Investigations of a Micro- Tangential-Jet Film Cooling Scheme on Gas Turbine Components," Ph.D.Thesis, Department of Mechanical and Industrial Engineering, Concordia University Montreal, Quebec, Canada, 2013.

[40]   D.R.Pedersen, E. R. G. Eckert, and R. J. Goldstein, "Film Cooling With Large Density Differences Between the Mainstream and the Secondary Fluid Measured by the Heat-Mass Transfer Analogy," ASME J. Heat Transf., vol. 99, pp. 620–627, 1977.

[41]   B. Johnson, W. Tian, K. Zhang, and H. Hu, "An experimental study of density ratio effects on the film cooling injection from discrete holes by using PIV and PSP techniques," Int. J. Heat Mass Transf., vol. 76, pp. 337–349, 2014.

## Biographical Information

**Bassam Ali Jubran** was educated at Cardiff University (formally University of Wales), Britain, graduating in 1980 with B.Sc. Honors degree in Mechanical Engineering. He obtained a Ph.D., also from the University of Wales, in 1984. Bassam has over 30 years of experience in leadership, research, and teaching positions. He is currently a Professor of Thermo-Fluid Engineering at Ryerson University and a member of the Professional Engineers of Ontario. Professor Jubran served as Editor-in-Chief of the Journal of Engineering Research and was on the editorial board of the International Journal of Low Carbon Technologies. He received the Hisham Hijjawi Award in the field of Energy and Informatics, 1997 and the Shoman Award for Young Arab Scientists (Engineering Sciences), 1994. Dr. Jubran has published more than 100 refereed Journal papers and over 50 conference proceedings papers. Bassam's lifetime funded research portfolio exceeds $5.5 million, with a research focus on energy and thermal management.

**Sana Abd Alsalam** received her B.Sc. degree in Aerospace Engineering from Tripoli University, Tripoli, Libya in 2005. She also got her M.Sc. degree in Aerospace Engineering from Tripoli University, Tripoli, Libya in 2013. Mrs. Abd Alsalam has more than six years of engineering work experience in Libyan Airlines, Tripoli, Libya. Sana is currently pursuing her Ph.D. degree at Ryerson University, Toronto, Canada wherein she joined the Aero-Thermal Management Laboratory group in September 2015. Her main research area of interest is in the numerical analysis of thermal and flow field of micro hole film cooling as well as sister holes film cooling for gas turbine cooling applications.